Finite Element model set-up of colorectal tissue for analyzing surgical scenarios

Robinson Guachi[1]*, Fabiano Bini[1], Michele Bici[1], Francesca Campana[1], Franco Marinozzi[1]

[1] Department of Mechanical and Aerospace Engineering, DIMA – Sapienza University of Rome, 00184, Rome, Italy;

* robinson.guachi@gmail.com;

Abstract *Finite Element Analysis (FEA) has gained an extensive application in the medical field, such as soft tissues simulations. In particular, colorectal simulations can be used to understand the interaction with the surrounding tissues, or with instruments used in surgical procedures. Although several works have been introduced considering small displacements, as a result of the forces exerted on adjacent tissues, FEA applied to colorectal surgical scenarios is still a challenge. Therefore, this work aims to provide a sensitivity analysis on three geometric models, taking in mind different bioengineering tasks. In this way, a set of simulations has been performed using three mechanical models named Linear Elastic, Hyper-Elastic with a Mooney-Rivlin material model, and Hyper-Elastic with a YEOH material model.*

Keyword Finite Element Analysis; Soft Tissues Simulation; Surface Modeling; Computer Assisted Surgical Planning.

Introduction

In the recent past, Finite Element Analysis (FEA) has increased its applications in medical field, in particular to make preoperative plans and simulations of surgery, [1]. Soft tissues simulations, such as colorectal simulation, may be adopted to understand the interaction with surrounding tissues, as well as the effect of instruments used in surgical procedures. In this way, FEA may improve the surgical procedure, also optimizing or designing new instruments for robot-assisted laparoscopic or other minimally invasive surgeries [2]. Moreover, FEA is a virtual prototyping tool for the preoperative plan, according to the particular characteristics of the patient involved in the surgery [3].

Modeling the mechanical behavior of tissues and reproducing geometrical conditions are of the utmost importance for the accuracy of a FEA. In this paper, we are going to discuss these topics applied to colorectal surgical scenarios. More in detail, we are going to investigate how material properties and geometrical changes of the organ will have effect on the strain-stress distributions achieved by FEA.

In the next Section, the paper introduces the state of the art concerning FEA in soft tissues and related investigation about material models that are suitable to capture their behavior. Section 3 presents the geometric models analyzed in the work and their FEA set-up, while Section 4 presents the achieved results. Three case studies are investigated in this paper, with the aim of simulating the interaction between a surgical instrument and part of the colorectal tissue. Finally, in Section 5 we discuss the conclusion and guidelines for future works.

Related works

To correctly evaluate stress-strain with FEA, it is necessary to know the mechanical behavior and soft tissue geometry. The mechanical properties of a given tissue can be measured either “in vivo” or “ex vivo”. In literature [4], the effects of different testing conditions were studied and an artificial environment was created to mimic the “in vivo” environment. Therefore, many laboratory tests have been performed to determine the mechanical properties of soft tissues in both people and animals [5]. Colon and surrounding tissues have a mechanical behavior that is non-linear visco-elastic [8], but, due to the difficulty to perform the laboratory tests, some works, as [6] and [10], have performed some mechanical behavior approximations from elastic-linear to hyperelastic material models.

Nevertheless, simplified material models, like for example an elastic-linear one, can be used in some bioengineering FEA according to its simulation goals. More in detail, elastic-linear model is applied for training of new surgeons through virtual reality. Hyperelastic models are necessary when major accuracy is requested in the stress-strain evaluation like in preoperative planning, to reproduce and understand phenomena as, for example, tissue detachment, implant analysis [3,11,12,13].

Considering colorectal tissue, studies based on destructive test have determined that, from the statistical point of view, the colorectal tissue can be assumed to be is an isotropic tissue [3]. In order to reduce the complexity problem, some authors assume a simplified mechanical behavior of the tissue, called Linear Elastic (LE). It provides a linear approximation of the stress-strain behavior through the Hook law. [3,7,14,15]

More accurate models, able to describe real tissue are Hyper-Elastic with a Mooney-Rivlin material model (HE-MR), and Hyper-Elastic with a YEOH material model (HE-Y). They are phenomenological material models used in FEA to analyse large deformations of materials, such as rubber [16]. Non linearity is captured by describing the stored energy in the reference volume unit of material, in terms of strains, through the invariants of the Green deformation tensor [17]. Figure 1 (taken from [9]) gives an overview of how HE-Y works in terms of force-displacement. In this case, non linearity is captured by a third-order polynomial that is based only on the first invariant, I_1, of the Green deformation tensor.

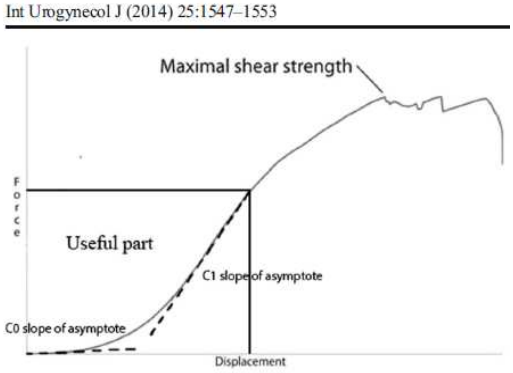

Figure 1. Mechanical behaviour of the tissue in its Hyperelastic approximation.

Table 1 provides information about material parameters, with corresponding meaning and material properties values, as derived by literature for colorectal simulations.

Table 1: Parameters used in the simulation of colorectal tissues.

Method	*Parameter*	*Description*
EL [10]	E=5.18 MPa	Young modulus
HE-MR [1]	C10=0.085 MPa C01=0.0565 MPa	Hyper-Elastic – Mooney-Rivlin
HE-Y [12]	C10=0.088 MPa C20=3.092 MPa C30=2.871 MPa	Hyper-Elastic - YEOH

Definition of the case studies

- ***Geometric models***

The case studies investigated in this paper represent two simplified geometric models and one real geometric model, which has been obtained from segmented Magnetic Resonance Imaging (MRI) images. All of them have lengths related with the anatomical data of the colorectal tissue of the closer area to the sigmoid colon.

MRI were acquired by means a 1.5 T scanner (Sonata Siemens, Erlangen, Germany), with a phased-array body surface coil. A 3D manual segmentation has been

processed by means of Slicer3D, version 4.5 [18], according to Data Imaging and Communications in Medicine (DICOM) procedures. Specifically, in order to obtain 3D images, the expert has to move the cursor through the boundary of the segmented region of interest and he can fill all the space enclosed in, by applying a set of reference-standard algorithms and graphical tools. The boundary was delineated by following the rule that a pixel belongs to the region of interest when it is included in at least two out of the three delineations drawn by the expert. Generally speaking, manual segmentation is employed when tumor and colorectal zone were revised with the assistance of radiologists before segmentation. In fact, recent studies focused on rectal cancer suggested that 3D anatomical imaging segmentation, obtained from DICOM of MRI, could contribute in the definition of the circumferential resection margins and in the pre-operative assessment of the tumor regression grade following chemo-radiation treatment [19].
From the acquired data, the length of the entire colon is about 1500 mm. For our analysis and simulations, we choose to take a part of it, placed in the zone between the sigmoid area and the rectum area. This part has length about 100 mm (7% of the entire colon). In this colorectal zone, the average outer diameter of the intestine is about 25 mm.
The first geometric model, Plane Surface (PS) (Figure 2), is the most simple, assuming the tissue as a planar surface. It is assumed to be completely in contact with the tool that simulates the surgical grasper. PS dimensions are 100 mm for length and $\frac{25}{2} \times \pi \approx 39{,}3\ mm$ for width (this value is found considering an ideal semi-cylinder with an outer diameter of 25 mm).

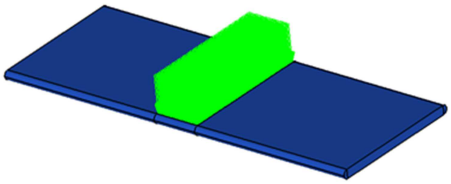

Figure 2: Plane Surface (PS), in blue, and related applied load, in green.

The second geometric model is a Cylindrical Surface (CS) (Figure 3). It is an idealization of the colorectal tissue geometry modeled with an outer diameter of 25mm and a length of 100 mm, as in the previous case. This model corresponds to a geometry in a position prior to the interaction with the surgical grasper, that, in the simulations, is assumed to be a rigid body.

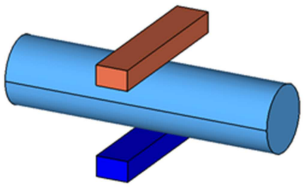

Figure 3: Cylindrical Surface (CS).

The third geometric model represents a real surface of colorectal tissue derived from MRI (MRIS), (Figure 4). The 3D model, as obtained by the segmentation, has been imported in CATIA to be checked and optimized. Outliers deletion and hole recovery were necessary to model, via NURBS, the colorectum surface, as shown in Figure 4. NURBS modeling has been made in CATIA, starting from the stl tesselation of the 3D model and adopting reverse engineering techniques for free-form modeling [20].

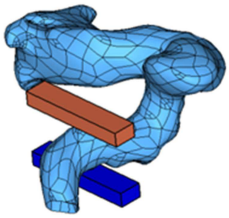

Figure 4: MRI Surface (MRIS).

- ***FEA set-up***

FEA has been carried out in the Hyperworks environment, through OptiStruct and RADIOSS solvers. OptiStruct has been used for the PS case study, taking into account the latest step of the real clamping process. It concerns with the compression of the soft tissue caused by the grasper tightening. RADIOSS has been used to analyse tissue deformation during surgical grasper motion in case of CS and MRIS case studies. According to this distinction, loads have been applied following two different schemes. The first one represents a distributed force acting like the grasper tightening (load#1); the second one is a force exerted on the tissue by the contact with the surgical grasper during its motion (load#2). The value used for load#1 and load#2 come from experimental data that recommend a value of $P = 8\frac{g}{mm^2}$ [21], suitable for manipulating soft tissues without tearing. CS and MRIS simulations are considered empty, since patient's preoperative plan asks for emptying digestive system before the surgical operation. Table 2 summarizes investigated conditions related to material models, solver and geometric models (the HE-Y model is not implemented in RADIOSS so CS and MRIS are analysed only with LE and HE-MR).

Table 2: Conditions of material models, solver and geometric models

Geometric model	*LE*	*HE-MR*	*HE-Y*	*Load condition*	*Solver*
PS	X	X	X	Load#1	OptiStruct
CS	X	X		Load#2	RADIOSS
MRIS	X	X		Load#2	RADIOSS

Boundary conditions, similar to real behaviour, are difficult to define. Support structures, such as ligaments and fasciae, are not clearly distinguishable from clinical images. In order to recreate constraints similar to the conditions on the tissue when performing colorectal surgery, simplification of the boundary conditions has been performed at the ends of the geometries, releasing rotations in all axes, and displacement along colon axial direction.

PS model has been discretized, in OptiStruct, using 3D elements (hexahedral elements) [5] (Figure 5a). CS and MRIS models were discretized, in RADIOSS, using Shell elements (quad, 4 nodes) [5] (Figure 5b and 5c). Shell elements have a wall thickness of approximately 1.2 mm, according to the data found in [5], which is considered constant throughout the entire geometry.

Since one of the goals of the paper is the understanding of mesh effects on stress-strain results, we have considered different lengths of elements, which directly influence in the number of elements used in each geometric model. With this, we can identify the minimum element length necessary to achieve reliable results with minor computation efforts. The number of elements, the corresponding element type and the element dimension are given in Table 3.

Table 3: Characteristics of the elements used in the different geometric models.

Type of Geometry	*Element dimension (mm)*	*Element Type*	*# of elements*
PS	4	Hexahedral	1900
	2	Hexahedral	3800
	1	Hexahedral	7600
CS	4	Shell	475
	2	Shell	1850
	1	Shell	7500
MRIS	4	Shell	2244
	2	Shell	6408
	1	Shell	23095

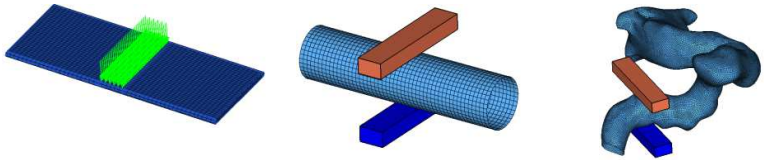

a) b) c)

Figure 5: Geometric model. a) Discretized PS with hexahedral elements; b) Discretized CS with Shell elements; c) Discretized MRIS with shell elements

To conclude the FEA set-up, we highlight that simulations made by RADIOSS obviously asked for hourglass checks, and contact definition. Hourglass was managed by QEPH shell formulation, recommended for high number of elements. Contact condition was provided by "type 7" card definition assuming the surgical grasper as rigid.

Experimental results

In this section we analyze the influence of material models on the FEA set-up, described in the previous section. Results are discussed according to the achieved stress-strain distributions.

- ***PS results***

FEA in 2D is often carried out with the aim of simplifying the geometric model, combined with a linear elastic approximation of the soft tissues mechanical behavior. Doing so, it reduces execution time and computational cost of the FEA. In the PS geometry, an applied load of P = 8gr / mm^2 [21] is used to analyse the behavior of the three types of material models.

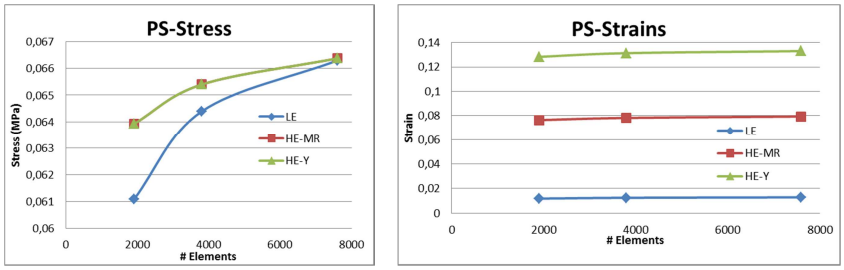

a) b)

Figure 6: PS sensibility respect to the length of the element and material model. a) Stress; b) Strain

Different behaviour between linear elastic and hyperelastic models is observed in Figure 6a, while HE-MR and HE-Y are the same. The similar behaviour of the two hyperelastic models indicates that, according to the load conditions imposed

in the PS case-study, the two models act similarly. (generally, for higher values of strain, HE-Y can fit better the real trends than HE-MR [16]).
The strain behavior varies notably changing the material models, as shown in in Figure 6b. The highest strain value is achieved with HE-Y, the lowest with LE. Therefore, it is clear that the linear elastic approximation represents a model stiffer than HE ones [17].
The effect of variation of elements' length (and consequently their number) is more evident for stress values. In Figure 6a, a trend of convergence can be seen for number of elements higher than 4000. In Figure 7, the contour-plot of the Von Mises equivalent stress is shown for the case of minimum length.

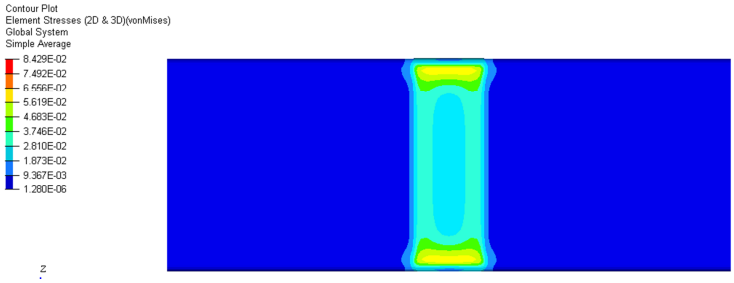

Figure 7: Color map of the stress distribution in the PS model (Stress in MPa).

This contour-plot describes the stress distribution in the tissue where the interaction with the surgical grasper occurs. A stress concentration is shown at the free-edges of the model. The distribution is coherent for each of the three material models.

- ***CS results***

In FEA, simplified 3D geometry may help to understand the phenomena that are presented in real geometries. Previous works on FEA of soft tissues [3] recommend to study a simplified geometry, uniform and symmetrical as possible, in order to avoid errors or wrong analysis caused by geometrical irregularities and also to develop procedures not influenced by specific cases.
The CS case study represents a simplified model of the MRIS model of colorectal tissue with the set-up conditions established in Section 3. In this case, an explicit FEA simulation is made by RADIOSS, taking into account contact and dynamics during grasping.

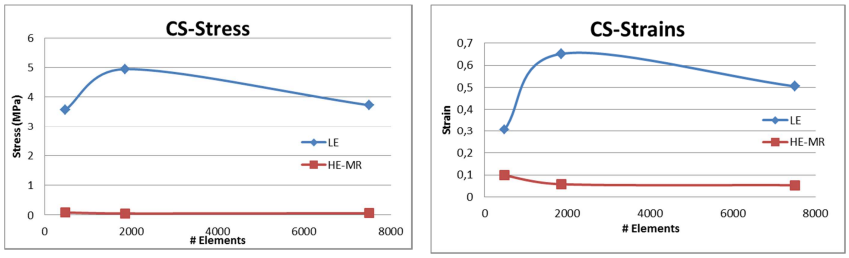

a) b)

Figure 8: CS sensibility respect to the length of the element and material model. a) Stress; b) Strain.

Figure 8 shows some differences in stress and strain passing from LE to HE-MR, while element length does not provide relevant changes, nor trends of convergence like in PS. LE results are higher than HE-MR both for stress and strain. To better understand this phenomenon, we have analysed the instant in which the tissue starts the contact with in surgical grasper. Figure 9a shows the deformed shape in that instant with a particular in the central zone. Figure 9b represents stress contour plot in case of HE-MR. We can observe that the stress gradient starts from the lateral zone (free edges) of the CS model and not in the central zone where the contact with the grasper starts. This phenomenon is caused by the material high flexibility, which involves a local displacement of the tissue before generation of stress in the same area. In the LE model for CS case, as reported in Figure 9c, we can observe an opposite effect in respect to the HE-MR model. Due to a more rigid behaviour, local consented displacements before the generation of stress are lower than the HE-MR model. This produces the appearance of stress gradient in the area where the contact with the surgical grasper starts. This gives evidence that this phenomenon is directly connected to the material behaviour proving that LE model has a stiffer behaviour than the HE-MR one. Due to this, stress can be overestimated utilising a LE model. This phenomenon produces the same effect in strain distribution. Obtained results with HE-MR model for stress and strain values in PS and CS case are comparable.

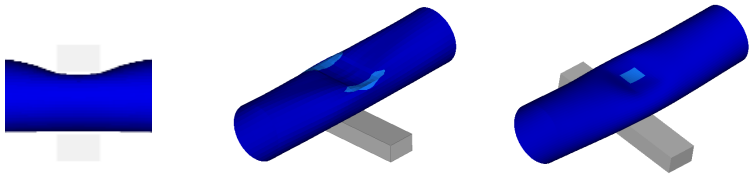

a) b) c)

Figure 9: Stress gradient. a) Particular of the deformed shape at the contact instant; b) Stress gradient with the HE-MR model (blue zone with stress < 0.006 MPa, cyan zone with stress between 0.006 and 0.01 MPa); c). Stress gradient with the LE model (blue zone with stress < 0.4 MPa, cyan zone with stress between 0.4 and 0.8 MPa)

- ***MRIS results***

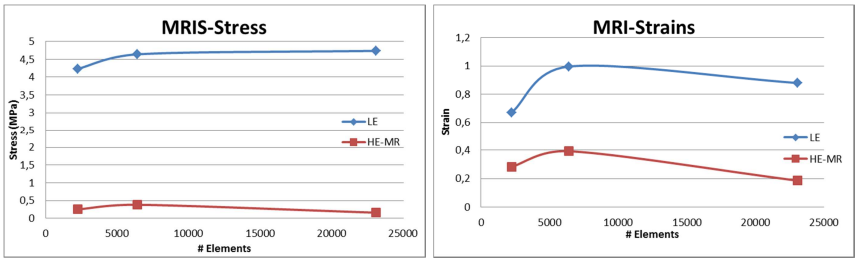

a) **b)**

Figure 10: Stress and strain results. a) Stress in different material models; b) Strain in different material models.

In this case, the behaviour obtained between the two types of material models corresponds to the effect already described for CS.

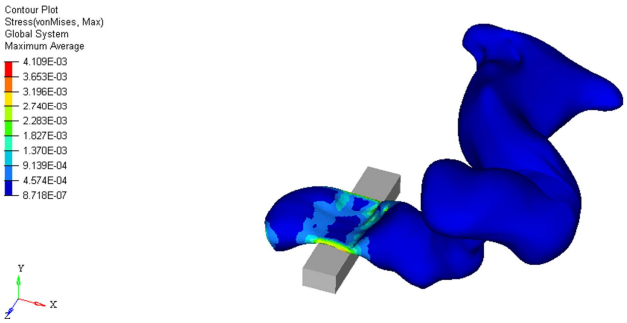

Figure 11: Stress contour-map in the MRIS geometric model

The results obtained for the HE-MR model in MRIS case are comparable with ones for PS and CS models. Taking into account that the maximum FEA stress is 0.08 MPa and ultimate strength 0.85MPa [10], it would be said that no damage is generated in the tissue with the pressure exerted by the instrument during tightening operations.

Conclusion

The three models here evaluated result applicable, with a good level of reliability, in increasing deformation field. However, more in particular, LE is more rigid under the same load conditions, followed by HE-MR and HE-Y, which implies that for the analysis of complex geometries (free-form shapes), such as colorectal tis-

sue, the linear elastic model may fail to predict the field of tensions and deformations, thus overestimating strains on the tissue.

These results are useful in the clinical field: for the evaluation of the feedback force on the instrument, for configuration of training devices based on haptic sensors and for combined kinetic-structural simulations of the instrument.

References

[1] Shi HJ (2007) Finite element modeling of soft tissue deformation. Dissertations & Theses, University of Louisville.

[2] Xu, K., Goldman, R., Ding, J. and Allen, P. (2009). System design of an insertable robotic effector platform for single port access (SPA) surgery. Intelligent Robots and Systems, 2009. IROS 2009. IEEE/RSJ International Conference on, pp.5546-5552.

[3] Mayeur, O., Witz, J., Lecomte, P., Brieu, M., Cosson, M. and Miller, K. (2015). Influence of Geometry and Mechanical Properties on the Accuracy of Patient-Specific Simulation of Women Pelvic Floor. Annals of Biomedical Engineering, 44(1), pp.202-212

[4] Ottensmeyer, M.P., Kerdok, A.E., Howe, R.D., Dawson, S.L. (2004). The effects of testing environment on the viscoelastic properties of soft tissues. Int'l Symposium on Medical Simulation. Lecture Notes in Computer Science 3078; Cambridge, USA. pp. 9–18

[5] Liao, D., Zhao, J. and Gregersen, H. (2010). 3d Mechanical properties of the partially obstructed guinea pig small intestine. Journal of Biomechanics, 43(11), pp.2079-2086.

[6] Rubod, C., Brieu, M., Cosson, M., Rivaux, G., Clay, J., de Landsheere, L. and Gabriel, B. (2012). Biomechanical Properties of Human Pelvic Organs. Urology, 79(4), pp.968.e17-968.e22.

[7] Qiao, Y., Pan, E., Chakravarthula, S., Han, F., Liang, J. and Gudlavalleti, S. (2005). Measurement of mechanical properties of rectal wall. Journal of Materials Science: Materials in Medicine, 16(2), pp.183-188.

[8] Chantereau, P., Brieu, M., Kammal, M., Farthmann, J., Gabriel, B. and Cosson, M. (2014). Mechanical properties of pelvic soft tissue of young women and impact of aging. International Urogynecology Journal, 25(11), pp.1547-1553.

[9] Egorov, V., Schastlivtsev, I., Prut, E., Baranov, A. and Turusov, R. (2002). Mechanical properties of the human gastrointestinal tract. Journal of Biomechanics, 35(10), pp.1417-1425.

[10] Christensen, M., Oberg, K. and Wolchok, J. (2015). Tensile properties of the rectal and sigmoid colon: a comparative analysis of human and porcine tissue. SpringerPlus, 4(1).

[11] Jeanditgautier, E., Mayeur, O., Brieu, M., Lamblin, G., Rubod, C. and Cosson, M. (2016). Mobility and stress analysis of different surgical simulations during a sacral colpopexy, using a finite element model of the pelvic system. International Urogynecology Journal, 27(6), pp.951-957.

[12] Chen, Z., Joli, P., Feng, Z., Rahim, M., Pirró, N. and Bellemare, M. (2015). Female patient-specific finite element modeling of pelvic organ prolapse (POP). Journal of Biomechanics, 48(2), pp.238-245.

[13] Pan, J., Chang, J., Yang, X., Zhang, J., Qureshi, T., Howell, R. and Hickish, T. (2011). Graphic and haptic simulation system for virtual laparoscopic rectum surgery. The International Journal of Medical Robotics and Computer Assisted Surgery, 7(3), pp.304-317.

[14] Dequidt, J., Marchal, M., Duriez, C., Kerien, E. and Cotin, S. (2008). Interactive Simulation of Embolization Coils: Modeling and Experimental Validation. Medical Image Computing and Computer-Assisted Intervention – MICCAI 2008, pp.695-702.

[15] Rao, G. V., C. Rubod, M. Brieu, N. Bhatnagar, and M. Cosson. Experiments and FE modeling for the study of prolapsed in the pelvic system. Comp. Meth. Biomech. Bio-med. Eng. 13(3):349–357, 2010. Simulation of normal pelvic mobilities in building an MRI-validated biomechanical model

[16] Sasso, M., Palmieri, G., Chiappini, G. and Amodio, D. (2008). Characterization of hyperelastic rubber-like materials by biaxial and uniaxial stretching tests based on optical methods. Polymer Testing, 27(8), pp.995-1004.

[17] Shahzad, M., Kamran, A., Siddiqui, M. and Farhan, M. (2015). Mechanical Characterization and FE Modelling of a Hyperelastic Material. Materials research,18(5), pp. 918-924.

[18] Fedorov, A., Beichel, R., Kalpathy-Cramer, J., Finet, J., Fillion-Robin, J., Pujol, S., Bauer, C., Jennings, D., Fennessy, F., Sonka, M., Buatti, J., Aylward, S., Miller, J., Pieper, S. and Kikinis, R. (2012). 3D Slicer as an image computing platform for the Quantitative Imaging Network. Magnetic Resonance Imaging, 30(9), pp.1323-1341.

[19] Lorenzon, L., Bini, F., Balducci, G., Ferri, M., Salvi, P. and Marinozzi, F. (2015). Laparoscopic versus robotic-assisted colectomy and rectal resection: a systematic review and meta-analysis. International Journal of Colorectal Disease, 31(2), pp.161-173.

[20] Campbell, R.J., Flynn, P.J. (2001). A Survey Of Free-Form Object Representation and Recognition Techniques, Computer Vision and Image Understanding, Volume 81, Issue 2, Pages 166-210, ISSN 1077-3142, http://dx.doi.org/10.1006/cviu.2000.0889

[21] Baker, R., Foote, J., Kemmeter, P., Brady, R., Vroegop, T. and Serveld, M. (2004). The Science of Stapling and Leaks. Obesity Surgery, 14(10), pp.1290-1298.

[22] Zienkiewicz, O. (1977). The finite element method. 1st ed. Maidenhead: McGraw-Hill.